

Critical Flow Centrality Measures on Interdependent Networks with Time-Varying Demands

James Bryan Williams

University of Toronto, Department of Computer Science, Canada

Abstract

This paper describes a novel method for allowing urban planners and municipal engineers to identify critical components of interdependent infrastructure networks whose attributes vary over time. The method is based on critical flow analysis, wherein system components are ranked by their role in facilitating the flow of resources to critical locations. The intent of the method is to support decision making by providing a means by which stakeholders can reason about the way in which changes in supply, demand, or network capacity can alter the distribution of critical flows within an urban environment. Individual infrastructure systems are modeled as networks that can be linked to one another by physical and geospatial dependencies. A simple instantiation of the method is presented and evaluated on a district-scale model of a city that contains water and electricity networks. The paper also discusses two forms of reliability analysis based on critical flows: a composite measure incorporating edge reliability, and a variation on standard component failure/degradation analysis.

Keywords: Component importance measures, Centrality measures, Complex systems, Network science, Infrastructure reliability

1. Introduction

This paper presents a novel method for identifying critical components in interdependent, urban infrastructure systems. The ultimate goal of the research is to develop a decision support tool that allows urban planners and municipal engineers to reason about risks introduced by interventions (e.g., zoning changes, maintenance activities). The paper demonstrates that standard network analysis techniques can be combined with criticality and reliability metrics in order to define a composite method that provides useful information for decision makers.

9 Although the method described in this work can be used in a variety of contexts,
10 the paper focuses on urban infrastructure systems (excluding transport). Residents
11 of cities depend on infrastructure systems to deliver not only physical resources
12 such as water and gas, but also a range of social goods ranging from education
13 to healthcare. Disruptions in the delivery of resources and/or services can have
14 extremely deleterious consequences, particularly for critical locations such as
15 hospitals. Methods for identifying the infrastructure components that supply
16 critical locations with resources could be used in several activities, including
17 maintenance scheduling, disaster recovery, and zoning.

18 Infrastructure systems can be disrupted in numerous ways, including deliberate
19 attacks, component failures, and natural disasters. Much of the existing research
20 on critical infrastructure protection, for instance, has focused on protecting infras-
21 tructures against damage due to extreme weather or deliberate attacks [1, 2, 3].
22 Component failure has been studied extensively in the field of reliability engineer-
23 ing (e.g., [4]) and in the various engineering disciplines (e.g., water [5], drainage
24 [6], electricity [7], telecommunications [8], and transportation [9]). Disruption of
25 networks has also been considered in operations research (e.g., [10]), computer
26 science (e.g., [11, 12]), network reliability (e.g., [13, 14]), graph theory (e.g.,
27 [15, 16]), and network science (e.g., [17]).

28 While the method presented in this paper can represent disruptions, it was
29 designed to accommodate a broader set of issues. In addition to severe, short
30 term events (e.g., natural disasters), infrastructure systems are influenced by a
31 variety of factors, including: (1) *population growth*, which typically results in
32 increased demands; (2) *component degradation*, which can introduce new capacity
33 constraints; (3) *maintenance activities*, which can shift flows of resources from
34 one route to another, and; (4) *planning interventions* (e.g., the development of new
35 residential subdivisions), which can have effects both on system topology and on
36 demand patterns.

37 In order to accommodate this diverse set of scenarios, the method includes
38 three major features that, in combination, distinguish it from prior art: (1) lo-
39 cations are annotated with *criticality ratings*, allowing distinctions to be drawn
40 between different types of facility; (2) infrastructure systems may be connected
41 via geospatial and physical *dependencies*; (3) system attributes (e.g., demand for
42 resources) are modeled as *time series*, permitting the user to reason about the
43 impacts of interventions or disruptions over different time scales.

44 The structure of this paper is as follows. Section 2 provides useful background
45 information, while Section 3 introduces the methodology used in this paper. Sec-
46 tion 4 provides an evaluation of the methodology on a district-scale model of a

city. Section 5 discusses two forms of reliability analysis that can be combined with critical flow measures. The paper closes with suggestions for future research.

2. Background

The method in this paper can be viewed as a combination of techniques from network science and critical infrastructure protection. The fundamental building block is a *component importance measure* ("CIM") (e.g., [18], [19], [20]) that estimates the degree to which a given component participates in the delivery of resources to critical locations. Before discussing the method in detail, a quick discussion of relevant background material is required.

2.1. Network Science and Centrality Measures

Networks are a common choice of modeling mechanism in many fields, and critical infrastructure protection is no exception (see [1]). For example, many approaches to infrastructure vulnerability and resilience make use of techniques from network science. From the perspective of the current paper, the most important of these techniques are the *centrality measures*, which are used to identify the most central components in a network (see [21, 22, 23]).

Numerous centrality measures exist [24], the most intuitive of which are: (1) *nearness measures*, which determine a given component's centrality by means of its proximity to other components, and; (2) *betweenness measures*, which deem components to be central to the extent to which they stand between other components as intermediaries. These categories contain measures that largely focus on network topology; in contrast, *dynamical measures* take into account various dynamical processes taking place on the network.

The progenitor of the method used in this paper is *flow centrality* [25]. Consider a simple network with nodes V and links E . A node v is considered to be *between* other nodes u and w to the extent that the maximum flow between u and w depends on v . Nodes are deemed central to the extent that they facilitate maximum flow.

Stated formally, for $u, v, w \in V$, let $m_{u,w}$ be the maximum flow between u and w , and let $m_{u,w}(v)$ be the maximum flow between u and w that depends on v . Then the **flow centrality** ("FC") of a node $v \in V$ is the degree to which the maximum flow between all unordered pairs of nodes depends on v :

$$C^F(v) = \sum_{u \neq w \neq v} m_{u,w}(v) \quad (1)$$

2.2. Interdependent Infrastructures

Infrastructure systems are typically coupled to the extent that the failure of components in one system can cause failures in connected systems [26]. These *interdependent* systems are typically more fragile than solitary systems [27], with additional failure modes (e.g., *cascading failures* [28]) that can be quite complex. For example, water distribution systems impose much greater cascading damage on other systems than they receive in return [29], and they seem to display a greater propensity to initiate cascading failure in other systems [30].

Various research communities have advocated an integrated view of infrastructure systems, and a growing body of work is available on interdependencies (e.g., [31, 32]). For instance, homeland security initiatives following the September 11th terrorist attacks in the United States spurred numerous efforts addressing infrastructure interdependencies (e.g., [33]). Overviews of techniques for the modeling and simulating interdependent critical infrastructure systems may be found in several places, including [34].

2.3. Modeling Interdependent Infrastructures with Networks

One approach to analyzing interdependent infrastructure systems involves modeling them as *interdependent networks* [32]. Interdependent (or *multilayer* [35]) networks have received increasing amounts of attention of late, particularly from the physics and network science communities. A recent survey paper can be found in [36], while books on the topic are readily available (e.g., [37, 38, 32, 39, 40, 35]).

To be precise, a network A is **dependent** on network B if the state of B can influence the state of A [41] (see also [42]). Dependencies can be classified as follows [30]:¹

1. **Physical dependencies**, in which the state of A is affected by the material outputs/flows of B
2. **Geospatial dependencies**, in which certain components of A and B are in such close spatial proximity such that local events can affect both networks;
3. **Informational dependencies**, in which A and B are connected by *information and communications technology* ("ICT");
4. **Social dependencies**, in which A affects B along social dimensions;
5. **Procedural dependencies**, where A affects B on the basis of organizational or regulatory structures, and;

¹Alternative classifications appear in [43, 44].

107 **6. Financial dependencies**, where market conditions, financial crises and other
108 economic events allow one network to affect another.

109 There are many ways to represent these dependencies in network models, a dis-
110 cussion of which is beyond the scope of the paper.

111 2.4. *Finding Critical Components in Interdependent Networks*

112 Numerous researchers have proposed methods for identifying critical compo-
113 nents in interdependent networks. Typical examples are described below:

- 114 • Apostolakis and Lemon [45] evaluate the vulnerability of geospatially inter-
115 dependent infrastructure systems (gas, water, electric) by identifying **critical**
116 **locations** — geographical points that are susceptible to attack. Each system
117 is represented as a directed network in which vertices can represent not just
118 junctions but also physical features (e.g., manhole covers). Co-location of
119 assets (e.g., shared service tunnels) is modeled by allowing vertices from
120 one graph to appear in another. (Physical dependencies, such as the use of
121 electricity by the water system, are not modeled).

122 In their approach, a set of attack scenarios is identified and the networks
123 are analyzed in order to identify *minimal cut sets* (see [7]). The resulting
124 vulnerabilities are prioritized by: (1) the degree to which the targets are
125 accessible to the attacker (i.e., susceptibility), and; (2) the value of the
126 targets from the standpoint of the decision-maker, calculated by summing
127 their expected disutilities. The susceptibility and value are combined to
128 yield a **vulnerability category** — one of five colors ranging from green to
129 red.

- 130 • Lee et al. [43] provide a method for prioritizing service restoration activities
131 in an interdependent system-of-systems. Each independent system is repre-
132 sented as a flow network that carries commodities, composed of edges and
133 vertices that may both have capacity constraints. Dependencies are modeled
134 as additional constraints in a mixed integer network flow model. In addition
135 to geospatial and physical dependencies, they allow *shared dependencies*
136 (i.e., for multi-commodity flow networks) and *exclusive-or dependencies*
137 (i.e., to allow flow on a multi-commodity network to be restricted to one
138 type of commodity at a time).

- 139 • Duenas-Osorio et al. [46] study the interdependency of electricity and
140 water systems from a topological standpoint. Both geospatial and physical

dependencies are modeled, with the water system requiring electricity for pumps, lift stations, and control units. Conditional probability distributions are used to model potential failures of water system components given failure of electricity system components. Three types of vertex removal strategies are used to model disruptions; for each such disruption, a set of metrics are calculated: (1) nodal degree; (2) characteristic path length [47]; (3) clustering coefficient [48], and; redundancy ratio. Flows of water or electricity are not modeled.

- Buldyrev et al. [26] examine the impact of electricity system disruptions on the internet. Geospatial dependencies are modeled by assigning each internet server to the closest power station. Disruptions are initiated by removing power stations and tracking resulting nodal failures — in particular, a node v is considered to be failed if: (1) all of v 's neighboring nodes are failed, or; (2) the geospatially coupled node in the electricity network is failed. Nodes are ranked according to the consequences of removal. The authors argue that disruption of a small number of nodes in the electricity system is sufficient to provide cascading failures in the internet network.

- Galvan and Agarwal [49] perform vulnerability analysis on interdependent infrastructures by examining the impact of disruptions. Each infrastructure is represented as a flow network with a unique resource type. In each iteration of the analysis, a single node is selected for failure (disruption). After recomputing the flow solution, the algorithm identifies every node that is in violation of capacity constraints. These latter nodes are then disabled and the process repeats itself until no more failures occur.

The authors introduce a new vulnerability metric X_1 , defined as the fraction of nodes that fail after the first step of the cascading failure process. After using X_1 to rank nodes, they compare the results against traditional centrality measures (i.e., nodal degree, the flow value for the non-disrupted solution, and network efficiency).

- Svendsen and Wolthusen examine interdependent critical infrastructures in a series of papers [50, 51, 52, 53]. Their models represent multiple concurrent types of dependencies, categorized at a high level into *storable* and *non-storable* types. Each vertex v in a network can act as a producer or consumer of up to m different resources, and for each such resource v has a corresponding buffer. The authors investigate numerous issues, including the behaviour of systems with cyclic interdependencies.

177 3. Methodology

178 The goal of this work is to explore means by which urban planners, municipal
179 engineers and other decision makers can identify critical components of interde-
180 pendent infrastructure networks. When embodied in software, such methods can
181 be used to support decision makers engaged in maintenance scheduling, zoning,
182 capacity planning, or other activities related to municipal infrastructure.

183 3.1. Overview

184 The paper provides an example of such a method, based on a centrality measure
185 that combines classical flow centrality [25] with concepts from critical infrastruc-
186 ture systems (e.g., [45]). The perspective in the paper is *resource-based*, focusing
187 on the routes by which resources are delivered to consumers. Components are
188 deemed critical to the extent that they are involved in facilitating the flow of
189 resources to critical locations.

190 Computation of the centrality measure, *critical flow centrality* (“CFC”), can
191 be accomplished in several ways (see [54]). In the current paper, a discrete-valued
192 approach is taken in which: (1) an infrastructure system is represented as a flow-
193 network; (2) demands, capacities, and supply limits are given as integers, and;
194 (3) each demand node in the network is assigned a real-valued criticality rating.
195 Network flows are simulated with a standard maximum flow algorithm; once a
196 flow has been defined, a search-based algorithm computes expected contribution
197 of each component to the critical flow within the network.

198 Since infrastructure networks are not independent of each other, physical and
199 geospatial dependencies may be introduced between individual infrastructures.
200 The most important of these for the present paper are *physical dependencies* in
201 which resources provided by one system (e.g., electricity) are used by another
202 system (e.g., water pumps). One of the main contributions of the paper is to show
203 how CFC values can be propagated from one infrastructure system to another.

204 The method is demonstrated by applying it to a district-level model of a city.
205 Each lot has a type, a criticality rating, and a set of demand curves (time series) for
206 resources. For reasons of brevity, only two infrastructure systems (electricity and
207 water) are shown. The simple method provided in this paper also assumes that the
208 physical dependencies between individual infrastructures are acyclic.

209 The main thrust of the demonstration is to show that: (1) the computation
210 of CFC values can be performed efficiently, enabling their use in interactive GIS
211 applications; (2) CFC values can correctly propagate between system models,

212 and; (3) CFC computations can be integrated with standard reliability measures to
213 provide a composite view of a system.

214 The CFC measure itself is completely general, requiring only a flow solution
215 and a network topology. The method presented in this paper uses the same (dis-
216 crete) algorithms to compute values for each individual infrastructure system –
217 namely, (1) an integer-valued maximum-flow algorithm to approximate resource
218 flow within infrastructures, and; (2) a modified graph-search algorithm to compute
219 CFC values. These design choices are for ease of explanation, and more sophis-
220 ticated, heterogeneous systems can be accommodated. One can model a water
221 system using hydraulic techniques [55], for example, coupling it to an electricity
222 system that is simulated using its own domain-specific methods. Given a flow so-
223 lution and network topology, CFC values can be computed by using Markov-chain
224 Monte Carlo or random walks (see [54] for details).

225 3.1.1. *Integration with GIS*

226 This work was motivated by the problem of providing adequate decision sup-
227 port for urban planning. For instance, densification of urban areas is accompanied
228 by greater demand for resources; the increased demand could: (1) violate capacity
229 constraints, as in the case of the London sewer systems [56, 57], or; (2) threaten
230 the ability of a legacy infrastructure system to reliably deliver services to critical
231 locations such as hospitals and transportation hubs. Urban planners could benefit
232 from tools that allow them to visualize the impacts of land-use decisions on the
233 provision of critical resources and/or services.

234 Effective modeling of integrated infrastructure systems requires more than a
235 static, single-perspective approach. Management of disruption (and prevention of
236 cascading failures) requires an understanding of system dynamics [58]. Further-
237 more, any model used to study the disruption of interdependent infrastructures
238 needs to support two different perspectives [43]: (1) a ‘system-of-systems’ view
239 that focuses on dependencies, and; (2) a traditional view of each individual system
240 that is familiar to managers/specialists.

241 One means of providing infrastructure models that support multiple perspec-
242 tives is through the use of *geographical information systems* (“GIS”) software.
243 In fact, the critical information protection community has begun to use GIS as a
244 platform for resilience and vulnerability analysis [59]. For this reason, the method
245 described in this paper was explicitly designed for integration within GIS software.

246 3.1.2. Data Sources

247 Two major challenges arise when data sources are considered. First, data on
248 infrastructure systems does not always exist, and particularly not in a form that
249 permits detailed analysis of interdependencies. Second, infrastructure systems
250 in many countries (e.g., the United States power grid) are not under the control
251 of a single entity [58], making the data collection process difficult. The lack of
252 information on infrastructure assets has motivated some researchers to develop
253 techniques for inferring asset locations from proxy data sources (e.g., [60, 61]).

254 The model used in this paper is a mixture of synthetic and empirical com-
255 ponents. The basic topology (i.e., road and parcel structure) was taken from
256 downtown Toronto, albeit the boundaries were simplified in order to make dia-
257 grams feasible and to convey the basic method clearly. Resource demand profiles
258 (e.g., hourly water consumption for hospitals) were taken from empirical studies
259 and from municipal utilities.

260 3.1.3. Implementation

261 The sample method was implemented directly in C++ and OpenGL. Road and
262 building information was obtained from OpenStreetMaps, imported into ESRI
263 CityEngine, and edited manually to remove artifacts. Custom python scripts were
264 used to export the road network topology, block/lot geometry, and building shapes
265 from CityEngine to *Extensible Markup Language* ("XML") files. Infrastructure
266 systems were created manually using the application's editing functionality. Lastly,
267 the diagrams shown in this paper were generated by exporting model geometry
268 directly to *Scalable Vector Graphics* ("SVG") format.

269 3.2. Modeling Approach

270 This section discusses the building blocks of the simplified model, includ-
271 ing: (1) the network representation; (2) time series representation of supply and
272 demand; (3) criticality ratings, and; (4) inter-system dependencies.

273 3.3. Network Representation

274 An individual infrastructure system is modeled as a weighted, capacitated, flow
275 network $G = \langle V, E \rangle$ where G is a set of nodes, $E \subseteq V \times V$ is a set of edges:

- 276 • each node $v \in G.V$ has Euclidean **coordinate** $\vec{w}(v) = (v_x, v_y, v_z) \in \mathbb{R}^3$, as
277 well as an (optional) capacity constraint $c(v) \in \mathbb{N}$.
- 278 • each edge $e = (v_i, v_j) \in G.E$ has a **capacity** $c(e) \in \mathbb{N}$, a **flow** $f(e) \in \mathbb{N}$,
279 and a **length** $l(e) \in \mathbb{R}$ defined as $\|\vec{w}(v_i) - \vec{w}(v_j)\|_2$.

280 Note that each network G is a *multi-graph* in which multiple edges may connect a
 281 given pair of nodes, allowing for redundant (fallback) connections. Bi-directional
 282 relationships, cycles, and self-loops are all permitted.

283 A network G contains both source (supply) and sink (demand) nodes. The
 284 set of **source nodes** is $V_S = \{s_1, s_2, \dots, s_p\} \subseteq V$, and the set of **demand nodes**
 285 is $V_D = \{d_1, d_2, \dots, d_k\} \subseteq V$. All other nodes are called *transmission nodes*.
 286 Multi-functional nodes are supported using a standard maximum flow reduction
 287 (as described in Section 3.8.1).

288 A **flow** on G is a real-valued function $f : E \rightarrow \mathbb{R}$ on G 's edges that obeys three
 289 flow properties:

- 290 1. **Capacity Constraints:** for all $e = (v_i, v_j) \in E$, we have $f(e) \leq c(e)$.
- 291 2. **Skew Symmetry:** for all $e = (v_i, v_j) \in E$, we have $f((v_i, v_j)) = -f((v_j, v_i))$.
- 292 3. **Flow Conservation:** for all transmission nodes $v_t \in V - (V_D \cup V_S)$, we have
 293 $\sum_{v \in V} f((v_t, v)) = 0$.

294 Each network G supports a single type of resource/commodity, unlike the multi-
 295 commodity approach in [52]. The **value of a flow** is defined as the flow exiting
 296 the source nodes: $|f| = \sum_{v \in V} \sum_{s \in S} f(s, v)$.

297 3.4. Supply Constraints and Demand Distributions

298 Supply constraints and resource demands are represented as discrete, integer-
 299 valued *time series* (see [62]). (While capacities can also be represented as time
 300 series, the demonstration assumes node and edge capacities are static.) For simplic-
 301 ity, each time series is assumed to be regularly sampled at times $t_i \in T = [0, \infty]$.
 302 They can be interpreted as the output of functions:

- 303 • Each supply node $v \in V_S$ may be assigned an optional **supply constraint**
 304 **function** $f_v^s(t) : T \rightarrow \mathbb{N}^+$ that gives the maximum amount of resource that
 305 may be supplied from v at time t .
- 306 • Each demand node $d \in V_D$ has a mandatory **demand function** $\delta_d(t) : T \rightarrow$
 307 \mathbb{N}^+ that gives the amount of flow required by node d at time t .

308 An **assignment** to a network involves specifying functions (time series) for all rele-
 309 vant nodes. Computations on the network (e.g., network flow solutions, criticality
 310 measures) are performed for each time $t_i \in T$. Values from previous time steps
 311 t_k may be used as input for computing values in the current time step t_i (where
 312 $t_k < t_i$). This permits the method to represent *delays* in resource utilization.

3.5. Criticality Ratings

A **criticality function** $cr : V_D \rightarrow \mathbb{R}$ maps demand nodes $d \in V_D$ to a **criticality rating** $cr(d)$. Although it is possible to use *binary* (e.g., critical, non-critical) or *categorical* (e.g., low, medium, high) representations, this paper focuses on the *continuous* variant in which criticality ratings take on values between 0 and 1.

3.6. Interdependencies

A *system-of-systems* (“SoS”) model consists of a set of k infrastructure systems $\mathcal{S} = \{S_1, S_2, \dots, S_k\}$. As shown in **Figure 1**, two types of dependencies are permitted between pairs of elements from \mathcal{S} :

1. **geospatial dependencies**, which arise when elements from network A are *co-located* with those from network B .
2. **physical dependencies**, wherein elements in network A require resources flowing through network B .

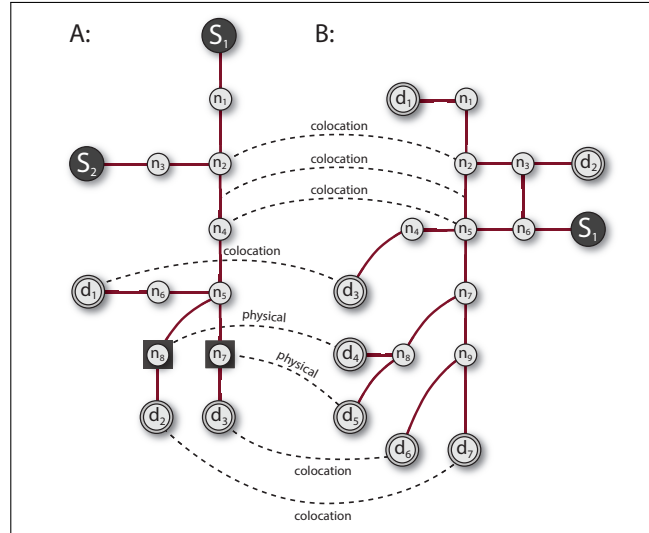


Fig. 1. Two independent infrastructure systems (A) and (B), linked by geospatial and physical (e.g., flow-related) dependencies.

Dependencies are represented as *interlinks* between individual infrastructure networks [35]. In contrast to [45], nodes from one network S_i do not appear directly in another network S_j . This design choice makes it easier to integrate disparate modeling methods for each individual infrastructure system (see [63]).

330 Interlinks representing physical dependencies are implemented with the use of
 331 *interconnection records*. Referring to **Figure 2**, let S_1 represent a water distribution
 332 system, and let S_2 represent an electricity system. A dependency between water
 333 node $v_1 \in S_1$ and electricity node $v_2 \in S_2$ is represented by an **interconnection**
 334 **record** $IR(v_1, v_2)$. The amount of resource R demanded of S_2 by v_1 (e.g., the
 335 amount of electricity required to operate a given water pump) is given by a function
 336 $f^R : S_1.V \rightarrow \mathbb{R}$. For instance, a pump at v_1 might demand a constant amount of
 337 electricity per unit time, or it may require power proportional to the flow $f(v_1)$
 338 through v_1 (e.g., $f^R(v) = cf(v)$). *Delays* can be accommodated by deferring this
 339 demand to later time steps.

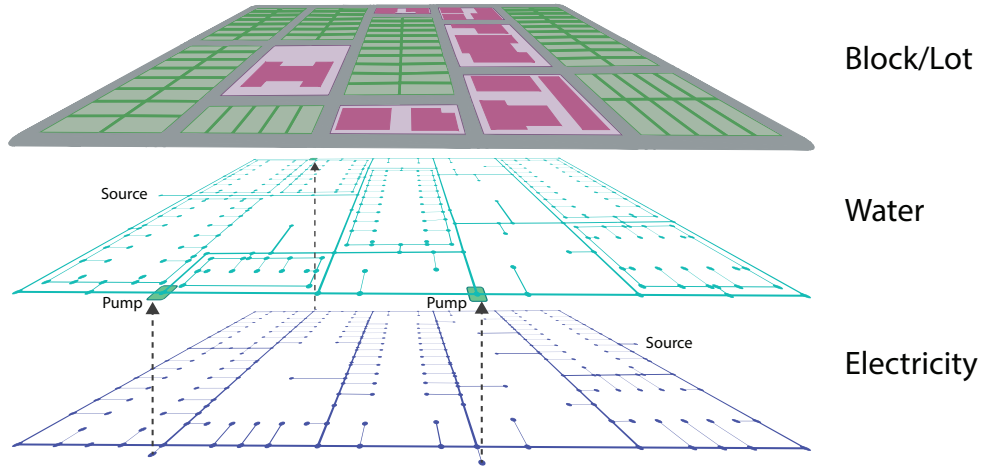


Fig. 2. Infrastructure model with two layers, showing resource flow between water pumps and electricity nodes.

340 Dependencies between network elements imply dependencies between sys-
 341 tems. If an interconnection record exists that maps elements of S_1 to elements
 342 of S_2 , we say that S_1 is **physically dependent** on S_2 , represented as $S_1 \rightarrow S_2$.
 343 Mutual dependency between systems makes the computational task more diffi-
 344 cult. The methods of Svendsen and Wolthusen (e.g., [52]) accommodate mutual
 345 dependencies using multi-commodity flows, but this approach does not allow for
 346 infrastructure-specific network representations and solution methods.

347 In this paper, the set of physical (resource) dependencies between systems in
 348 \mathcal{S} is taken to form a *directed, acyclic graph* (“DAG”) \mathcal{G} that can be ordered with a
 349 topological sort (see [64]). In contrast, geospatial dependencies are not restricted
 350 in such a fashion.

351 3.7. Critical Flow Centrality

The **Critical Flow Centrality** (“CFC”) measure reflects the degree to which a given component facilitates the flow of resources to critical locations. Recall that the **flow** in network G (given assignment A) is the aggregate of all flows reaching the demand nodes:

$$F_A(G) = \sum_{d \in D} f_A(d) \quad (2)$$

The **critical flow** in network G given assignment A is the set of flows reaching the demand nodes, weighted by criticality:

$$F_A^C(G) = \sum_{d \in D} f_A(d) c_r(d) \quad (3)$$

A component c (i.e., node or edge) is deemed to be important to the extent that it carries critical flow. Let $f_A(c, d)$ be the flow that reaches $d \in D$ from c given assignment A , and let $E[f_A(c, d)]$ be its expectation. Then the **critical flow centrality** (“CFC”) of component c under assignment A is:

$$C^{CF}(c) = \sum_{d \in V_D} c_r(d) E[f_A(c, d)]$$

This quantity may be normalized by the critical flow $F_A^C(G)$:

$$C'^{CF}(c) = \frac{C^{CF}(c)}{F_A^C(G)} = \frac{\sum_{d \in D} c_r(d) E[f_A(c, d)]}{\sum_{d \in D} c_r(d) f_A(d)} \quad (4)$$

352 Computing the CFC thus reduces to computing the probability $p(d|c)$ that
 353 a unit of commodity passing through component c ends up in demand node d .
 354 While there are numerous ways to accomplish this task (e.g., Markov chains), this
 355 paper uses a discrete, search-based approach.

356 For each time step t , a flow solution $F(t)$ is generated represented in a **sec-**
 357 **ondary graph** G' . This is an adjacency-list representation of the stochastic tran-
 358 sition matrix; every vertex v in G' maintains an *outgoing edge list* in which each
 359 edge is labeled with the probability that a unit of flow travels down that edge.

360 Each edge e and non-demand node v in G' have a *data structure* (i.e., *map*) that
 361 tracks the set of demand nodes reachable from them. Each entry in a map contains
 362 a tuple $(d, P(d|c_{map}))$ giving the probability that a unit of flow passing through
 363 reaches demand node d from the map’s parent component c_{map} . The collection of
 364 all such maps contains the information required to compute Equation 4.

365 The algorithm proceeds by performing a reverse DFS on G' for each demand
 366 node $d \in D$, computing the probability that each edge or non-demand node sends
 367 flow to d . A given node or edge may be visited multiple times in the course of
 368 the search, requiring care to avoid pushing superfluous probability. (This method
 369 does not, however, work for graphs G' that contain cycles).

```

Function ComputeProbabilities( $G'$ )
  Data:  $G'$ , a graph with components  $(V, E)$  and absorbing nodes
            $D \subseteq V$ .
  foreach  $d \in D$  do
    | ReverseSearch( $G'$ ,  $d$ )
  end

Function ReverseSearch( $G'$ ,  $d$ )
  Data:  $G'$ , as above.
  Data:  $d$ , an absorbing node.
  Var excess[]          // array of numbers  $\in [0, 1]$  of size  $|V|$ 
  Var stack
  excess[ $d$ .ID] = 1
  stack.push( $d$ )
  while stack not empty do
    Var curNode = stack.pop()
    Var amt = excess[curNode.ID]    // amount of probability
    to push
    foreach incoming edge curEdge of curNode do
      | curEdge.map.IncrementOrAddProbability( $d$ .ID, amt)
      | excess[curEdge.src.ID] = amt * curEdge.probability
      | stack.push(curEdge.src)
    end
    curNode.map.IncrementOrAddProbability( $d$ .ID, amt)
    excess[curNode.ID] = 0
  end

```

Algorithm 1: Probability Calculation.

370 Helper variable *excess* is a lookup table containing probability values for each
 371 node. The *IncrementOrAddProbability*() function updates the estimate of $P(d|c)$
 372 stored in the map of component c . The lookup table and variable *amt* are used to
 373 avoid problems with overlapping paths.

374 On typical infrastructure networks, **Algorithm 1** has time and space com-
 375 plexity of $O(|V|^2)$. Each map stores up to $|D|$ entries, leading to $O((|V| + |E|)|D|)$
 376 in storage space. The time required to perform the search for a given demand
 377 node is $O(|V| + |E|)$, yielding a total time of $O((|V| + |E|)|D|)$ for the entire
 378 graph. However, infrastructure networks typically have $|V| \approx |E|$ and $|D| \lesssim \frac{1}{2}|V|$,
 379 yielding time and space complexity of $O(|V|^2)$.

380 The running time of the entire method is thus dominated by the flow generation
 381 step, which is typically more expensive than $O(|V|^2)$. The current paper used the
 382 Edmonds-Karp algorithm (see [64]) for simplicity, which is $O(|V|^2|E|)$ on general
 383 graphs and $O(|V|^3)$ on infrastructure networks. Although flows can be generated
 384 with a variety of techniques (e.g., simulation), the method in Algorithm 1 only
 385 applies if the transition graph G' is acyclic. Alternative methods (e.g., simulation,
 386 Markov chains) can be used if cycles are present.

387 3.8. An Algorithm for Interdependent Critical Flow Centrality

388 Given a model \mathcal{S} with interdependent sub-systems $S_1, S_2, S_3, \dots, S_n$, Algo-
 389 rithm 1 can be used to compute CFC values for all components in each S_i at each
 390 time step t . This is not sufficient, however, as physical dependencies must be
 391 accounted for. Resource demands and criticality ratings must be propagated from
 392 one sub-system to the other.

393 Computing the CFC for the entire model \mathcal{S} proceeds by computing the CFC
 394 for each individual infrastructure system in topological order. Dependencies are
 395 processed from one system to the next in each iteration, passing demands from
 396 higher-level layers to lower-level ones. **Algorithm 2** provides a high level overview:

Function *ComputeInterdependentCFC*(\mathcal{G})

Data: G , a graph with nodes $V_{\mathcal{G}} = S = \{S_1, S_2, \dots, S_k\}$ representing
 individual infrastructure systems, and edges $E_{\mathcal{G}}$ formed from
 physical dependencies between elements of $V_{\mathcal{G}}$.

ConvertNetworkRepresentation(\mathcal{G})

Var list \leftarrow *TopologicalSort*($V_{\mathcal{G}}$)

Var t \leftarrow 0

foreach $S_i \in$ list **do**

 | *ComputeSingleSystemCFC*(S_i)

end

Algorithm 2: Computing CFC for a set of interdependent infrastructures.

397

3.8.1. Converting Network Representations

As a pre-processing step, conversion of network representations is performed to transform each individual network S_i into a format compatible with maximum flow algorithms.

1. Nodes with demands are connected to a *supersink* node (see [64, 65]).
2. Source nodes are connected to a *supersource* node.
3. Nodes in network S_1 that require resources from network S_2 are represented in S_2 by corresponding demand nodes.

In the case of (3), the criticality for the nodes in S_1 is only available after the CFC for all non-demand nodes has been computed. Thus, the full computation for S_1 must be performed before any computations can be performed for S_2 . **Figure 3** provides an illustration of network conversion.

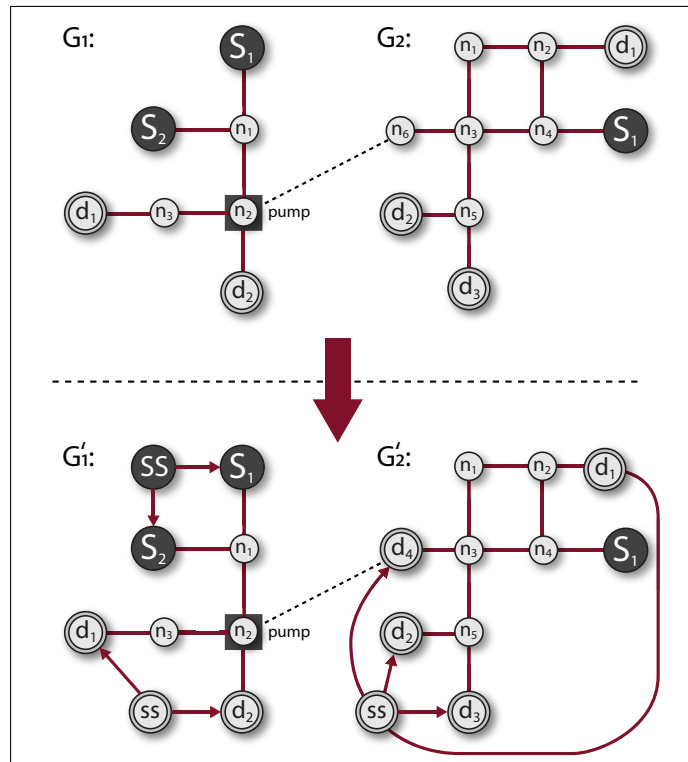


Fig. 3. Two independent infrastructure systems S_1 and S_2 , transformed into flow networks suitable for the Edmonds-Karp algorithm. Supersource ('SS') and supersink nodes ('ss') are added in the usual manner.

410 **3.8.2. Computing CFC Values for a Sub-system**

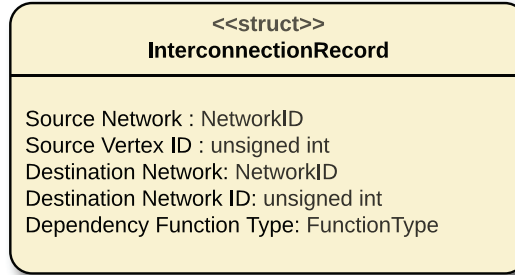
411 Computation of the CFC for sub-system S_i proceeds in two stages: (1) flow
 412 values and criticality values are propagated from other layers S_h ($h < i$) according
 413 to dependencies, and; (2) the CFC for S_i is computed using the technique discussed
 414 in **Section 3.7**. If layer S_i supplies layer S_h with resources (e.g., it is an electricity
 415 network that supplies power to water pumps), then resource demands for S_h appear
 416 in S_i 's network as sinks with appropriate demands. Topological ordering ensures
 417 that S_h 's criticality and flow values have been computed before S_i 's. **Algorithm 3**
 418 provides an overview of single layer CFC computation.

Function *ComputeSingleSystemCFC*(S_i)

PropagateValues(S_i)
 ComputeMaxFlow(S_i)
 ComputeCFC(S_i)

Algorithm 3: Computing the CFC for a set of interdependent systems.

419 Propagation of criticality and flow values proceeds by examining the set of
 420 relevant interconnection records:



421 An interconnection record $IR(v_1, v_2)$ (where $v_1 \in S_h, v_2 \in S_i$) indicates a
 422 physical (resource) dependency between systems S_h and S_i . Demand and criticality
 423 values for v_1 must be propagated to v_2 before the maximum flow and CFC can be
 424 computed for S_i .

425 **Algorithm 4** gives an overview of this process. Criticality values are copied
 426 directly, but the amount of resource that must be provided by v_2 to v_1 is determined
 427 by a function (e.g., the demand induced at v_2 is half of the flow at v_1).

```

Function PropagateValues( $S_i$ )
  foreach interconnection record  $IR(v_1, v_2)$  do
    if  $v_2 \in S_i.V$  then
       $v_2.demand \leftarrow CalculateResultingDemand((v_1, v_2))$ 
       $v_2.criticality \leftarrow v_1.criticality$ 
    end
  end

```

Algorithm 4: Propagation of resource demands.

428 **Figure 4** shows a water system and electricity system that are interlinked in
 429 two locations: pumps near the source of the water system are fed by electricity
 430 nodes labelled A and B . A flow solution was first computed for the water system,
 431 yielding flows of 6063 litres and 5973 liters at the pumps. The induced demand
 432 at nodes A and B of the electricity system are half of the flow – namely, 3031 and
 433 2986 units.

434 Note also that edges and vertices with no flow are shown in black. The existence
 435 of such elements is an artifact of the Edmonds-Karp algorithm [65, 64] used in
 436 this simple instantiation, and one that would be corrected by using domain-specific
 437 methods (e.g., hydraulic simulation [55]).

438 **Figure 5** shows the CFC values for the same interdependent infrastructure
 439 system under the same flow solution. Criticality levels (ranging from 0 to 1) are
 440 shown in white font for the buildings. (Lot criticality is fixed at 0.02, and elided
 441 for brevity).

442 Thanks to the propagation of both flow and criticality values from one network
 443 to the next, the criticality of the water pumps is appropriately represented in the
 444 criticality ratings of the electricity system. The electricity nodes A and B have
 445 inherited criticality values of 0.32 and 0.61 from the corresponding pump vertices
 446 in the water system; they require flow of 3031 and 2986 units, which the reader
 447 can verify by inspection are half of the flow values at the water pump.

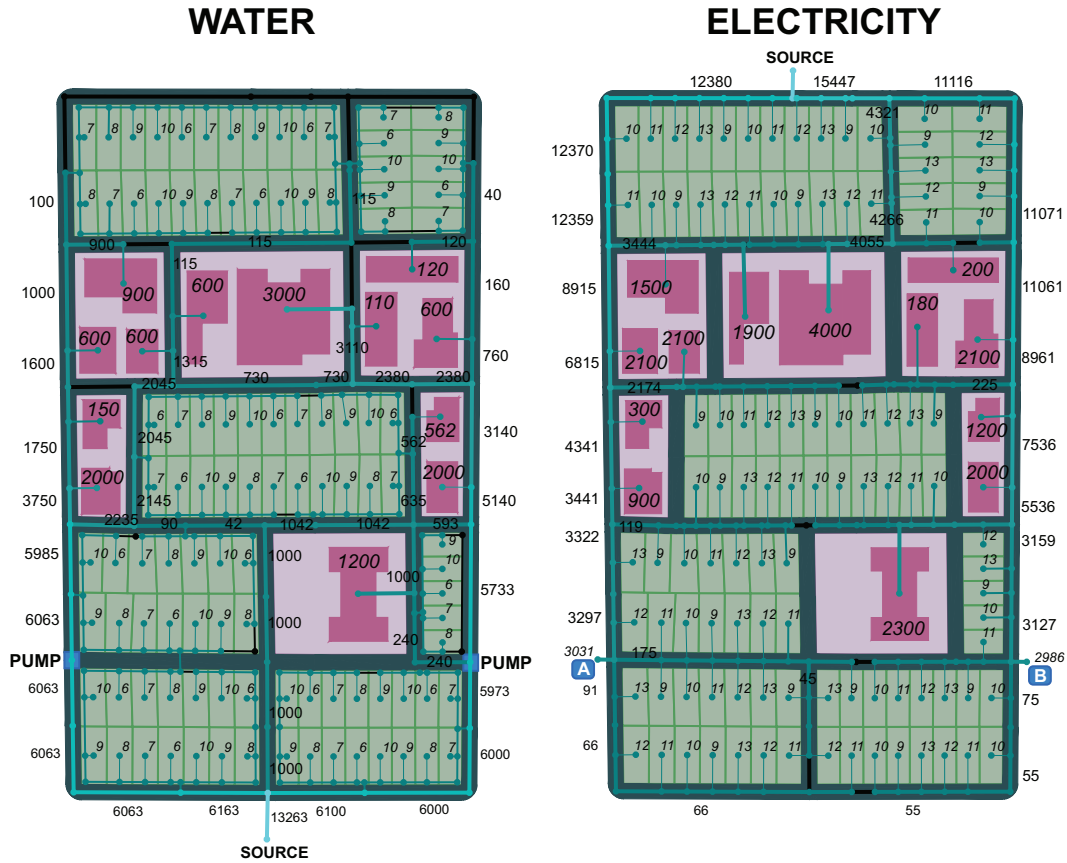


Fig. 4. Interdependent flows. Demand values are in italics while flow values are in regular font. Pumps in the water network are supplied with electricity by nodes A and B. Pumps require electricity proportional to half of their water flow. Black edges/vertices have zero flow.

While most of the critical demand in the model is for the hospital (criticality=1.0) and secondary school (criticality=0.6), the pumps create significant critical demand in otherwise non-critical regions of the model. **Figure 5** show that the electricity nodes supplying the pumps carry 16.7% and 8.7% of the total critical flow in the electricity network. It would be a poor decision to co-locate electrical assets with water assets when both are carrying highly critical flow.

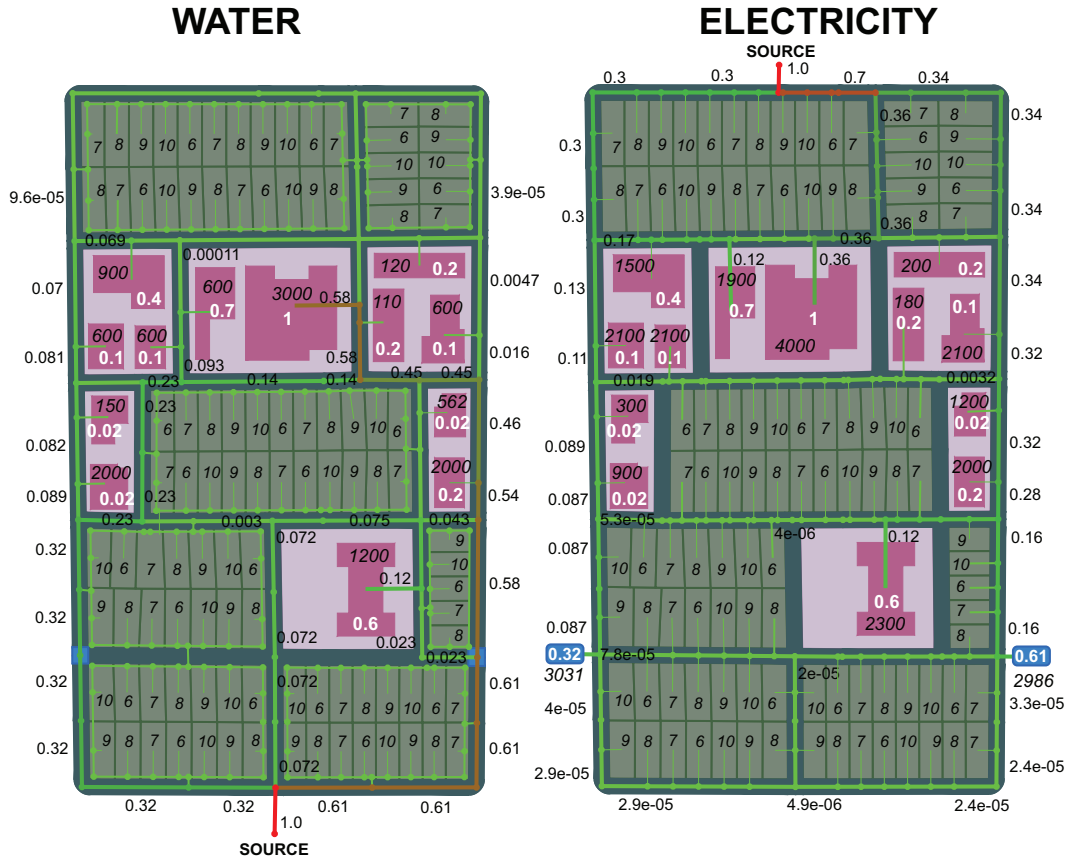


Fig. 5. (Normalized) critical flow centrality, computed from the flows in Figure 4. Demand values are in italics, CFC values are in regular font, and criticality ratings for buildings are in white. The electricity nodes that supply the water pumps are given criticality ratings of 0.32 and 0.61 and demands of 3031 and 2986 via Algorithm 4.

4. Evaluation

This section demonstrates the method by means of a district-level model of a city containing electricity and water systems. The simplicity of the model is for explanatory purposes; it is possible to use the method on models of greater complexity, provided that the physical interdependencies create a directed, acyclic graph.

Each building/lot in the model is given: (1) a *type* (e.g., hotel); (2) a time series representing *hourly demand for water*; (3) a time series representing *hourly demand for electricity*, and; (4) a *criticality rating* in the interval $[0, 1]$. Time

series are assumed to give average hourly demands over a 24-hour day. However, the method is general, and other scenarios could be supported, such as long-term (i.e., decadal) investigation of urban growth and its effect on capacity.

Time series data is assigned to buildings according to type (e.g., secondary school, restaurant), while lots are assigned time series randomly drawn from a library of typical residential demand curves. For simplicity, criticality ratings and vertex/edge capacities are assumed to be static, although they could easily be represented with their own time series.

Empirical data for different types of buildings in summer was obtained from several sources (e.g., water consumption data was sourced from the California Public Utilities Commission [66], electricity data from Ontario Power Generation). Examples of water demand curves appear in **Figure 6** below:

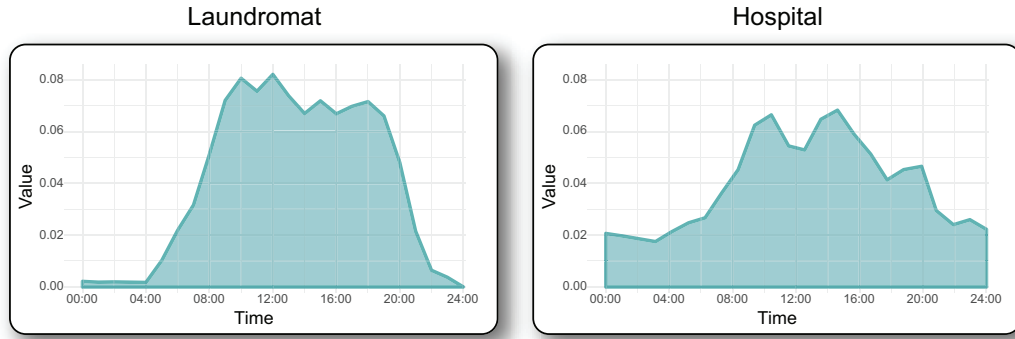


Fig. 6. Hourly time series showing water demands from a laundromat and hospital over an average day. The time series have been normalized to create a probability distribution. For use in the CFC method, these distributions are scaled by average water usage per day.

CFC values are computed for each time step $t \in [1, T]$ by loading the relevant time series data for t and executing **Algorithm 2**. An overview of the process is provided in **Algorithm 5**. Upon termination of this procedure, each node and edge in the interdependent system has a set of CFC values — one for each time step — that can be used in statistical analysis.

Figure 7 shows a graph of CFC values for the water network’s edges over the full 24-hour cycle:

The edge with a constant criticality rating of 1 is the lone edge incident to the source/reservoir. In general, the edges with significant criticality values tend to remain critical throughout the 24-hour cycle, with interesting behaviour happening during the middle of the day. Low criticality nodes become more critical during

Function *ComputeCriticaltyForTimeSeries*(\mathcal{G})

```

foreach  $t \in [1, T]$  do
    LoadDemands( $\mathcal{G}, t$ )
    ComputeInterdependentCFC( $\mathcal{G}$ )
end

```

Algorithm 5: Computing CFC on a system-of-systems with time-varying demands.

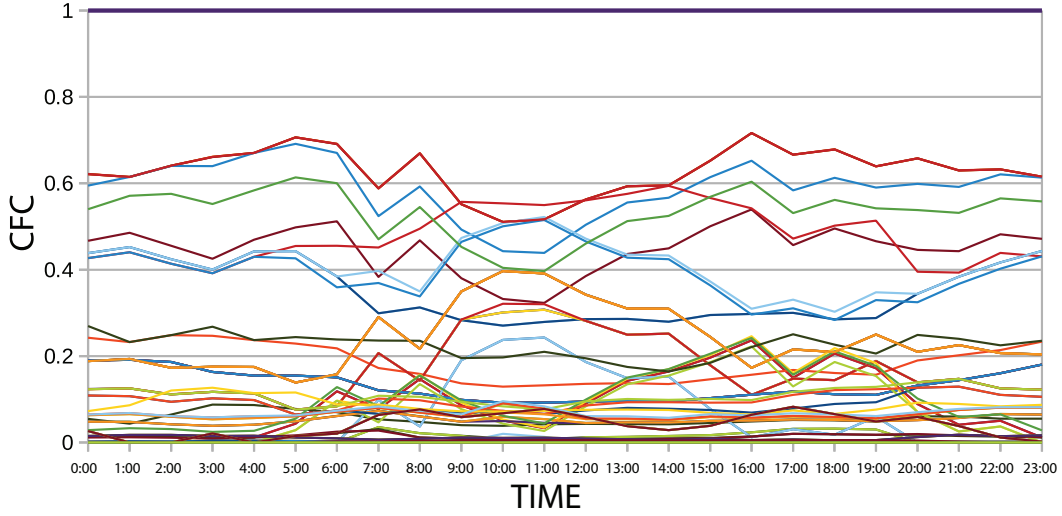


Fig. 7. CFC values for each edge in the water network.

486 mid-day, when significant water demand begins to push capacity constraints.

487 In contrast, the edges of the electricity network display a more stable distribu-
 488 tion. In **Figure 8**, one can clearly see that there are fewer intersections between
 489 lines in the plot of electricity edge criticality values. The edge to the single source
 490 node again has a constant criticality rating of 1, and the fluctuation in criticality
 491 values of other major edges is much less pronounced. This is likely a consequence
 492 of the fact that the demand on the electricity network does not tend to push capacity
 493 constraints as much as the demand on the water network.

To recap, Algorithm 5 results in a set of CFC values $CFC_t(c)$, where t is a timestep and c is a component. For instance, the output for the water system edges can be represented as a matrix CFC_{water}^e in which rows are timesteps and columns

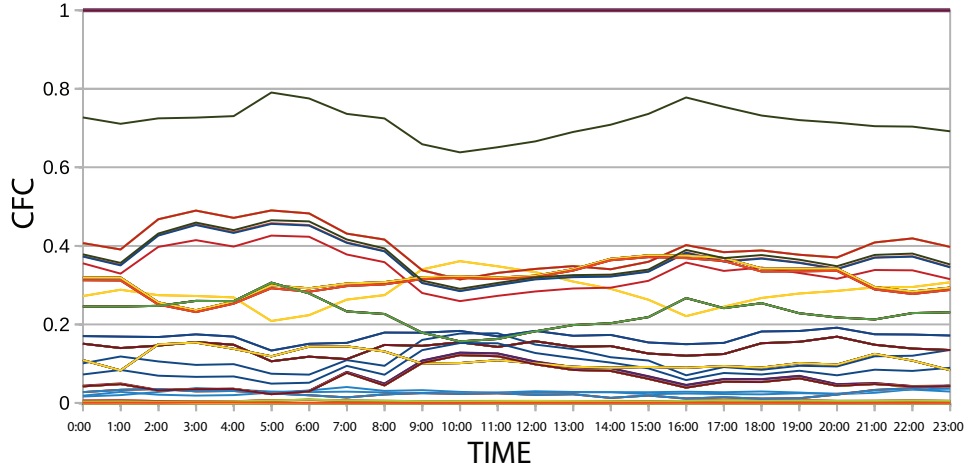


Fig. 8. CFC values for each edge in the electricity network.

are edges:

$$CFCte_{water}^e = \begin{vmatrix} CFC_1(e_1) & CFC_1(e_2) & CFC_1(e_3) & \dots & CFC_1(e_{|E|}) \\ CFC_2(e_1) & CFC_2(e_2) & CFC_2(e_3) & \dots & CFC_2(e_{|E|}) \\ \vdots & \vdots & \vdots & \ddots & \vdots \\ CFC_k(e_1) & CFC_k(e_2) & CFC_k(e_3) & \dots & CFC_k(e_{|E|}) \end{vmatrix}$$

494

495 One major issue not addressed by classical works on network centrality (e.g., [25])
 496 is the choice of ranking method for component measures taken at different times.
 497 The most intuitive approach to ranking the components is to take the *sample mean*
 498 of each column and to subsequently rank columns in descending order. This would
 499 be an appropriate strategy if each row of the matrix was a sample from the space of
 500 assignments (i.e., in a Monte Carlo approach) at a given time t . However, the rows
 501 in the matrix are assessments of the system at different points in time. The use of
 502 descriptive statistical measures (e.g., average, variance) elides system dynamics.
 503 The same is true of various other methods (e.g., spectral analysis, information
 504 theory) that might be employed to analyze the matrix.

505 The choice of ranking approach is dependent upon the purpose of analysis.
 506 Consider a long-term (e.g., multi-year) analysis that attempts to study the distri-
 507 bution of critical flow patterns in response to changing population densities and
 508 land-use patterns. In such a setting, the long-term behaviour of the system is of
 509 interest.

510 **Figure 9** displays a situation in which criticality curves for two different com-
 511 ponents have the same integral but completely different trends over time. For a
 512 long-term (decadal) analysis of infrastructure criticality, the component with the
 513 orange criticality curve is clearly the more important of the two. In this setting,
 514 some form of trend-based, multi-variable time series analysis is required.

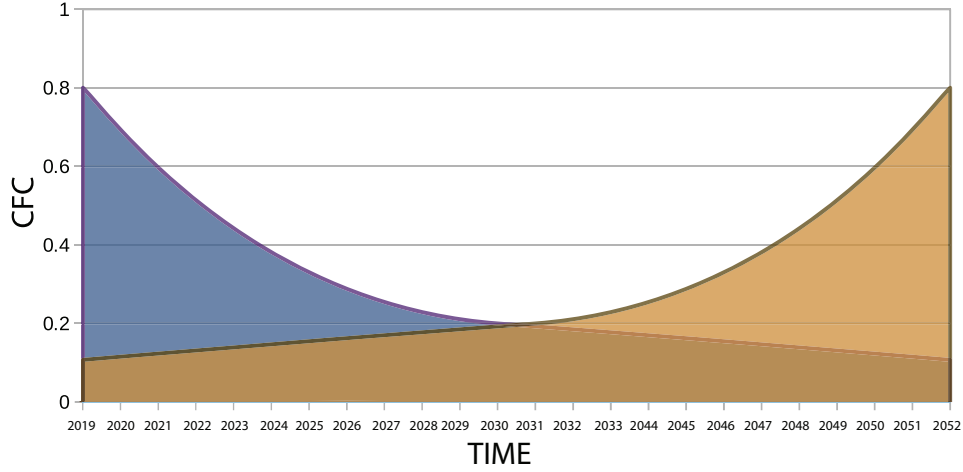


Fig. 9. Two components with similar integrals but different long term behavior.

515 Since the time series in this paper represent average demands in a *daily cycle*,
 516 components are ranked according to the *integral* of their CFC curve. Taking the
 517 water network edges as an example, a cubic spline is defined on the set of sample
 518 points $\{(CFC_1(e), CFC_2(e), \dots, CFC_k(e))\}$ corresponding to edge $e \in E$.

519 An integral is calculated from the cubic spline (as shown in **Figure 10**) and
 520 normalized by the maximum possible area $MAX_CFC \cdot (k - 1) = 1 \cdot 23 = 23$
 521 (recall that CFC values are already normalized, so that the maximum CFC at any
 522 time step is 1). The result is then assigned to the edge e as its *global CFC value*
 523 $CFC_G(e)$ for the entire time series. The set of all water network edges E is then
 524 ranked by sorting the edges according to their CFC_G values.

525 The same process is repeated for vertices, and for the other networks in the
 526 system-of-systems. Because of the way in which the critical flow centrality metric
 527 is defined, values for edges and vertices are commensurate, allowing a global
 528 ranking of all components in the interdependent system.

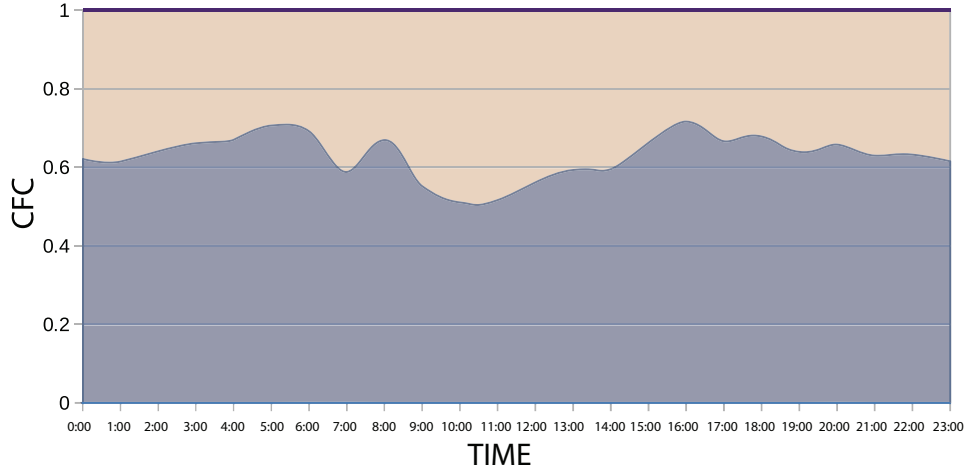


Fig. 10. Computing the global CFC value for a given component e . A cubic spline is overlaid on the CFC values for e . The integral of the spline (blue) is computed and normalized by the total area.

5. Reliability

This section demonstrates that the CFC measure may be combined with standard approaches to network reliability — namely, (1) edge reliability measures, and; (2) ‘leave one out’ failure analysis.

5.1. Edge Reliability

An arbitrary network model can be augmented by adding a **reliability function** $r : E \rightarrow [0, 1]$ that assigns edges $e \in E$ a **reliability rating** $r(e) \in [0, 1]$ [67]. One can combine this approach with CFC measures by creating a composite measure that estimates the joint reliability and criticality of a component. For instance, the (normalized) **Unreliable Critical Flow** (“UCF”) for an edge $e \in V$ is:

$$C'^{UCF}(e) = C'^{CF}(e)(1 - r(e))$$

where $C'^{CF}(e)$ is the normalized CFC for edge e . (The UCF is ‘normalized’ since values lie in the range $[0, 1]$, since $C'^{CF}(e)$ and $r(e)$ are both in $[0, 1]$.) Under this measure, components are important to the degree that they are: (1) unreliable, and; (2) instrumental for the delivery of resources to critical locations.

The computation of the UCF measure can be accomplished with a slight modification to the algorithm for the CFC. Instead of a static value $r(e)$, the reliability rating for a network component e can also be represented as a time

series $R_e = \{r_{e1}, r_{e2}, \dots, r_{ek}\}$. This allows the modeler to represent different processes (e.g., decreasing reliability of components over long time periods).

The UCF measures are computed for each timestep t using the CFC values and reliability ratings at t . The end result is a matrix in which entry (i, j) gives the UCF values for each edge e_j at timestep i . As in the case of the CFC, a cubic spline is overlaid on the values for each edge, creating an unreliability curve. After computing the integral and dividing it by the maximum possible area, the *global UCF value* for edge e is computed.

Geospatial dependencies between infrastructure components can be introduced into edge reliability analysis in a number of ways. For example, edges that are co-located (e.g., a water pipe and electricity pipe sharing the same service tunnel) could be forced to share the same reliability rating. Co-located components could also be assigned a reliability penalty that reflects the fact that component failures are no longer completely independent.

5.2. 'Leave One Out' Failure Analysis

CFC measures can also be used with a common form of reliability analysis in which components are deliberately failed or degraded (e.g., by reducing their capacity) in order to assess the effects on the system. A component e may have a high CFC value under a given assignment, but it may be the case that if e suffers a (partial) failure there are other routes (i.e., *fallbacks*) through which flow may travel in order to satisfy critical demand. **Figure 11** illustrates this situation:

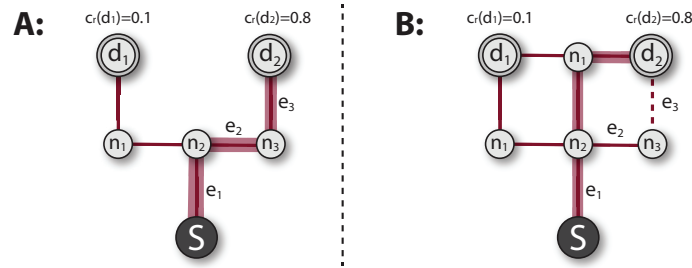


Fig. 11. Two networks with different behaviour in edge failure scenarios. Network A carries most of its critical flow through the path $\{e_1, e_2, e_3\}$. In case of edge failure, no alternative paths are available. Network B has a fallback route in case edge e_3 fails.

This form of failure analysis provides an indication of whether there are fallback routes that can supply critical flow in the event that a component e fails. If the failure of e consistently results in reduced critical flow across the entire network,

one can assume that e is even more critical than the CFC measure alone might suggest.

Algorithm 6 shows a high-level view of a procedure in which capacities of edges in a single infrastructure system are degraded one-at-a-time. For each time $t < T$, appropriate demands and criticality values are loaded into the graph. Then each edge $e \in E$ is considered in order, degrading its capacity and performing the CFC computation on the altered network. The critical flow is then used to create a *loss measure* that indicates the amount of critical flow that is lost when edge e is degraded. The **failure loss** $FL_t(e)$ for edge $e \in E$ at time t is:

$$FL_t(e) = 1 - \frac{\sum_{d \in V_D} f_A(d, t) c_r(d, t)}{\sum_{d \in V_D} \delta(d, t) c_r(d, t)}$$

where (recalling Section 3.4) V_D is the set of demand nodes in G , $\delta(d, t)$ is the demand at time t from demand node d , $f_A(d, t)$ is the actual flow to d at time t , and $c_r(d, t) \in [0, 1]$ is the criticality rating for d at t . Failure loss values range from 0 (no effect on resource delivery) to 1 (absolute disruption of resource delivery).

```

Function PerformEdgeFailureAnalysis( $S$ )
  foreach  $t \in [1, T]$  do
    LoadDemands( $S, t$ )
    foreach  $e \in E$  do
      Var originalCapacity  $\leftarrow$  e.capacity
      e.capacity  $\leftarrow$  Degrade(e.capacity)
      ComputeSingleSystemCFC( $S$ )
      ComputeFailureLoss( $S$ )
      e.capacity  $\leftarrow$  originalCapacity
    end
  end

```

Algorithm 6: Edge failure analysis on network S with time-varying demands.

The edge failure mechanism was tested on the network from **Figure 4** by degrading the capacity of each edge e to 0. (Demands and criticality ratings were the same as in previous sections.) The failure loss $FL_t(e)$ was computed for each edge e at each time $t \in [0, 23]$ and averaged over the 24 hour cycle to create an aggregate failure loss metric. The CFC values for each edge e were likewise averaged over the same time frame.

577 Figure 12 shows both the averaged CFC and averaged FL metrics for the
 578 edges of the water network. Two facts are immediately obvious. First, the vast
 579 majority of edges have negligible average CFC and FL values. These are typically
 580 low-capacity feeds from a residential street's water pipe to an individual lot/parcel.

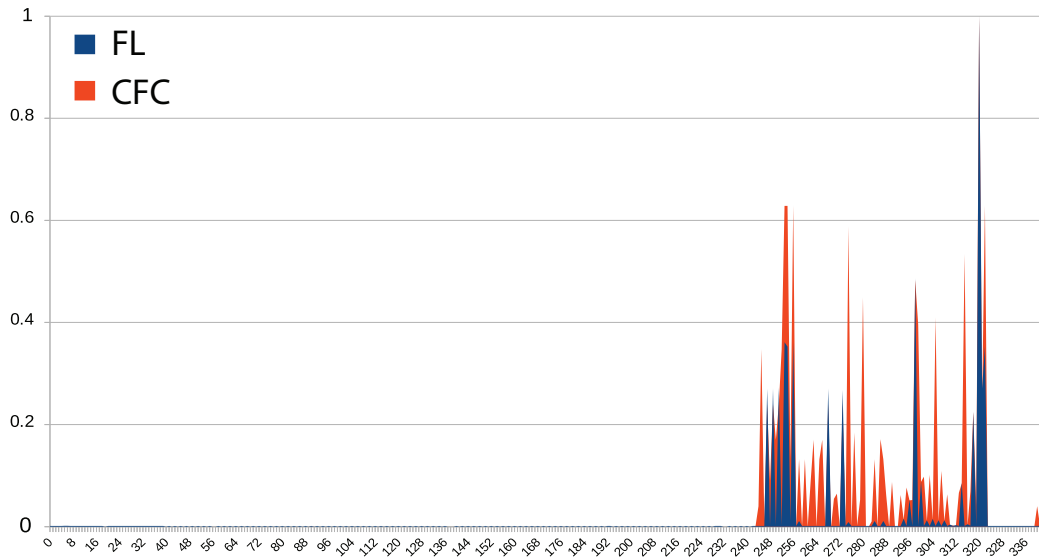


Fig. 12. Averaged *failure loss* (FL) and averaged *critical flow centrality* (CFC) on the edges of the water network in **Figure 4**, computed over a 24-hour period. The majority of edges (e.g., those that feed individual lots) have negligible FL and CFC values.

581 Second, a significant percentage of of those edges with high CFC ratings also
 582 have low FL values. Although these pipe segments carry a sizable amount of
 583 critical flow, alternative routes are available in case they should suffer individual
 584 failures. Examples include the pipes that define the loops around residential blocks;
 585 these loops are resistant to individual failure, since there are two paths from the
 586 entry point of the loop to any lot/parcel.

587 Of course, the main pipes from the reservoir have no backups, as demonstrated
 588 by the overlap of FL and CFC values for edge 320. In general, the correlation of FL
 589 and CFC is mildly significant but also somewhat misleading as a summary statistic.
 590 With a different network topology that included multiple sources and alternative
 591 paths, one would expect less correlation between the FL and CFC values, making
 592 the easily computable CFC a poor predictor of the consequences of edge failures.

593 5.3. *Reliability Integration Limitations and Assumptions*

594 The edge failure analysis presented above was subject to several simplifying
595 assumptions. First, geospatial dependencies were not included in the analysis for
596 reasons of brevity. Second, the failure loss analysis was performed on a single
597 network instead of a set of interdependent networks. Third, the reliability measures
598 could also incorporate component capacity, in order to capture the intuition that a
599 component nearing its maximum load is likely to be less reliable.

600 Fourth, the definition of the FL metric uses the aggregate of all demands at
601 the network's demand nodes as the normalizing factor. This is appropriate for a
602 network where all demands are satisfied in the baseline state, but it will overestimate
603 losses in networks which exhibit unsatisfied demand. For the scenario utilized in
604 this paper, however, this assumption is reasonable.

605 This method outlined in this work does not assume that the methods used to
606 model each layer are commensurate. That is, the electricity layer may be modeled
607 with one set of domain-specific techniques, while the water layer may be modeled
608 with another. All that is required is for each layer to provide a means of flow
609 computation and a basic network topology. This design decision, while useful
610 from a software engineering perspective, precludes the use of standard approaches
611 to modeling cascading failures.

612 To model physical dependencies and cascading failure in such a setting requires
613 the use of additional machinery. Component failure in the electricity system could
614 result in reduced power levels at the water pumps; this, in turn, could alter water
615 distribution flows, result in reduced electricity demand from other components of
616 the water system — thereby changing demand patterns for the electricity system.
617 Thus, the result is an *equilibrium problem* in which changes in one layer percolate
618 through other layers, and then back again. Solving such a problem is well beyond
619 the scope of this paper.

620 6. Conclusion

621 This paper demonstrated how component importance measures based on the
622 notion of critical flow may be applied to interdependent, urban infrastructure
623 systems. The motivation for the work was to provide urban planners and municipal
624 engineers with a method of reasoning about the impacts of interventions on the
625 flow of resources to critical locations. The main theme was that network analysis
626 techniques could be combined with criticality and reliability metrics in order to
627 produce composite methods that provide useful information to stakeholders.

628 The perspective of the method was resource-based, focusing on the ways in
629 which system components participate in the delivery of resources. Each individ-
630 ual infrastructure system S_i of a composite system S was represented as a flow
631 network with demands, capacities, supply limits, and criticality ratings. The paper
632 considered physical dependencies in which one subsystem S_i requires resources
633 from another subsystem S_j .

634 In the simple variant described in the paper, network flows and ‘critical flow
635 centrality’ (“CFC”) measures were computed using a discrete approach. More
636 sophisticated variants are possible, including the use of domain-specific simulation
637 techniques. For simplicity, the paper assumed that the subsystem dependencies
638 form a directed acyclic graph.

639 The method was demonstrated by use of a simple, district-scale model of a
640 city that contained electricity and water networks. Empirical data was used to
641 estimate resource consumption for different types of buildings, yielding a set of
642 demand curves that represent consumption in a 24-hour cycle. This decision
643 simplified the analysis, and allowed the use of integrals to compute a global CFC
644 value for the entire cycle. For the study of trends in infrastructure systems over
645 time, the integral-based aggregation would need to be supplanted by trend-based,
646 multi-variable time series analysis.

647 Despite the simplifying assumption, the simple method presented in the paper
648 satisfied the goals outlined in **Section 3.1**. First, the computation of CFC metrics
649 for an interdependent system can be computed efficiently. For a model $S =$
650 $\{S_1, S_2, \dots, S_k\}$ consisting of k subsystems, computation of CFC metrics for S
651 on typical infrastructure networks is $O(kV^2)$, where V is the average number of
652 nodes in the subsystems. This compares favorably with other centrality measures,
653 which can be $O(V^3)$ or greater.

654 Second, the demonstration showed that the basic method correctly propagates
655 resource demand, criticality ratings and CFC values between systems. Not only
656 are CFC values comparable across components within a given system, but they
657 are commensurable across systems – even in cases where disparate modeling
658 methodologies have been used.

659 Third, the paper showed how common network reliability approaches can be
660 combined with CFC measures to yield composite metrics. Edge reliability can be
661 directly integrated into the CFC framework by adding another attribute to the edges
662 and tweaking the CFC computation slightly. The paper also discussed edge failure
663 analysis, showing that a composite failure loss metric can be defined that gives
664 an indication of the availability of fallback routes for the delivery of resources to
665 critical locations.

Many avenues of future work remain, the most important of which is removing the restriction of \mathcal{G} to directed, acyclic graphs. To do so invites consideration of equilibrium concerns — changes in one network cause changes in others, altering flow distributions and demand patterns in complex ways. Providing solutions for this type of problem is well outside the scope of the present paper.

The instantiation of the CFC computation presented in both the current and previous papers are suitable for medium/long time horizons. The main culprit is the use of integer-valued representations for demands and capacity constraints. This decision, which was made in order to simplify the problem and avoid numerical instability, means that short term dynamics are difficult to represent. This precludes forms of analysis in which the rates of change (e.g., of flow) on system components may be analyzed. The use of floating point representations and domain-specific flow computation methods (e.g., simulation) will avoid this restriction.

Even with this restriction in place, there are still additional issues to be resolved. First, a more realistic flow mechanism (e.g., domain-specific methods) should replace the generic Edmonds-Karp algorithm that favors shortest paths (thereby introducing artifacts into the flow solution). Second, geospatial dependencies should be introduced into both the edge reliability and component failure analyses. Additional avenues of future research were hinted at throughout the paper.

7. Acknowledgements

Funding for this work was provided by an Ontario Research Fund — Research Excellence Round 7 grant for the “iCity: Urban Informatics for Sustainable Metropolitan Growth” project. The author wishes to thank Eric Miller, Mark Fox, Steve Easterbrook, and the rest of the researchers involved with the iCity project for the opportunity to work on problems outside of his existing areas of expertise.

References

- [1] T. G. Lewis, Critical Infrastructure Protection in Homeland Security: Defending a Networked Nation, Wiley-Interscience, 2006.
- [2] R. M. Clark, S. Hakim, A. Ostfeld, Handbook of Water and Wastewater Systems Protection, Springer, 2011.
- [3] J. Lopez, R. Setola, S. D. Wolthusen, Critical Infrastructure Protection: Information Infrastructure Models, Analysis, and Defense, Springer, 2012.

- 698 [4] A. Birolini, Reliability Engineering Theory and Practice, 5 ed., Springer,
699 Berlin Heidelberg, 2007.
- 700 [5] N. R. Council, Drinking Water Distribution Systems: Assessing and Reduc-
701 ing Risks, Technical Report, Committee on Public Water Supply Distribution
702 Systems: Assessing and Reducing Risks, 2006.
- 703 [6] D. Meijer, M. van Bijnen, J. Langeveld, H. Korving, J. Post, F. Clemens,
704 Identifying critical elements in sewer networks using graph-theory, Water
705 10 (2018).
- 706 [7] A. A. Chowdhury, D. O. Koval, Power Distribution System Reliability: Prac-
707 tical Methods and Applications, Wiley, Hoboken, New Jersey, 2009.
- 708 [8] M. G. Resende, P. M. Pardalos, Handbook of Optimization in Telecommu-
709 nications, Springer, New York, NY, 2006.
- 710 [9] M. A. P. Taylor, Vulnerability Analysis for Transportation Networks, Elsevier,
711 Amsterdam, Netherlands, 2017.
- 712 [10] M. T. Thai, P. M. Pardalos, Handbook of Optimization in Complex Networks:
713 Theory and Applications, volume 57, Springer, 2012.
- 714 [11] K. Wolter, A. Avritzer, M. Vieira, Resilience assessment and evaluation of
715 computing systems, Springer, 2012.
- 716 [12] R. S. Wilkov, Analysis and. Design of Reliable Computer Networks, IEEE
717 Transactions on Communications 20 (1972) 660–678.
- 718 [13] I. Gertsbakh, Y. Shpungin, Network Reliability and Resilience, Springer,
719 2011.
- 720 [14] S. K. Chaturvedi, Network Reliability: Measures and Evaluation, Scrivener
721 Publishing, Hoboken, New Jersey, 2016.
- 722 [15] B. Sudakov, V. Vu, Local resilience of graphs, Random Structures and
723 Algorithms 33 (2008) 409–433.
- 724 [16] M. Krivelevich, C. Lee, B. Sudakov, Resilient pancyclicity of random and
725 pseudo-random graphs, SIAM Journal on Discrete Mathematics 24 (2009)
726 1–17.

- [17] L. Dall'Asta, A. Barrat, M. Barthélemy, A. Vespignani, Vulnerability of weighted networks, *Journal of Statistical Mechanics: Theory and Experiment* (2006) P04006.
- [18] S. Dunn, S. M. Wilkinson, Identifying Critical Components in Infrastructure Networks Using Network Topology, *Journal of Infrastructure Systems* 19 (2012) 157–165.
- [19] C. D. Nicholson, K. Barker, J. E. Ramirez-Marquez, Flow-based vulnerability measures for network component importance: Experimentation with preparedness planning, *Reliability Engineering and System Safety* 145 (2016) 62–73.
- [20] Y. Almoghathawi, K. Barker, Component importance measures for interdependent infrastructure network resilience, *Computers and Industrial Engineering* 133 (2019) 153–164.
- [21] K. Stephenson, M. Zelen, Rethinking centrality: Methods and examples, *Social Networks* 11 (1989) 1–37.
- [22] V. Latora, V. Nicosia, G. Russo, *Complex Networks Principles, Methods and Applications*, Cambridge University Press, Cambridge (UK), 2017.
- [23] M. Curado, L. Tortosa, J. F. Vicent, G. Yeghikyan, Analysis and comparison of centrality measures applied to urban networks with data, *Journal of Computational Science* forthcoming (2020). URL: <https://doi.org/10.1016/j.jns.2019.116544>.
- [24] J. P. Scott, *Social Network Analysis: A Handbook*, SAGE Publications, London, UK, 2000.
- [25] L. C. Freeman, S. P. Borgatti, D. R. White, Centrality in valued graphs: A measure of betweenness based on network flow, *Social Networks* 13 (1991) 141–154.
- [26] S. V. Buldyrev, R. Parshani, G. Paul, H. E. Stanley, S. Havlin, Catastrophic cascade of failures in interdependent networks, *Nature* 464 (2010) 1025–1028.
- [27] A. Vespignani, Complex networks: The fragility of interdependency, *Nature* 464 (2010) 984–985.

- 758 [28] E. Zio, G. Sansavini, Modeling failure cascades in critical infrastructures with
759 physically-characterized components and interdependencies, in: ESREL
760 2010 Annual Conference, 2010, pp. 652–661.
- 761 [29] R. Zimmerman, C. E. Restrepo, The next step : quantifying infrastructure
762 interdependencies to improve security, *Int. J. Critical Infrastructures* 2 (2006)
763 215–230.
- 764 [30] W. Kröger, C. Nan, Addressing Interdependencies of Complex Technical
765 Networks, in: G. D’Agostino, A. Scala (Eds.), *Networks of Networks: The*
766 *Last Frontier of Complexity*, Springer, 2014, pp. 279–310.
- 767 [31] M. Papa, *Critical Infrastructure Protection II*, Springer, 2008.
- 768 [32] A. Garas, *Interconnected networks*, Springer, 2016.
- 769 [33] F. Petit, D. Verner, J. Phillips, L. P. Lewis, Critical Infrastructure Protec-
770 tion and Resilience—Integrating Interdependencies, in: A. J. Masys (Ed.),
771 *Security by Design*, Springer, 2018, pp. 193–219.
- 772 [34] M. Ouyang, Review on modeling and simulation of interdependent critical
773 infrastructure systems, *Reliability Engineering and System Safety* 121 (2014)
774 43–60.
- 775 [35] G. Bianconi, *Multilayer Networks: Structure and Function*, Oxford Univer-
776 sity Press, 2019.
- 777 [36] S. Boccaletti, G. Bianconi, R. Criado, C. I. Genio, The structure and dynamics
778 of multilayer networks, *Physics Reports* 544 (2014) 1–122.
- 779 [37] Per Hokstad, I. B. Utne, J. Vatn, *Risk and Interdependencies in Critical*
780 *Infrastructures: A Guideline for Analysis*, Springer, 2012.
- 781 [38] G. D’Agostino, A. Scala, *Networks of Networks: The Last Frontier of Com-*
782 *plexity*, Springer, 2014.
- 783 [39] H. Amini, K. G. Boroojeni, S. S. Iyengar, P. M. Pardalos, F. Blaabjerg, A. M.
784 Madni, *Sustainable Interdependent Networks: From Theory to Application*,
785 Springer, 2018.

- 786 [40] M. H. Amini, K. G. Boroojeni, S. S. Iyengar, P. M. Pardalos, F. Blaabjerg,
787 A. M. Madni, Sustainable Interdependent Networks II: From Smart Power
788 Grids to Intelligent Transportation Networks, Springer, 2019.
- 789 [41] S. M. Rinaldi, J. P. Peerenboom, T. K. Kelly, Identifying, understanding, and
790 analyzing critical infrastructure interdependencies, IEEE Control Systems
791 Magazine 21 (2001) 11–25.
- 792 [42] A. Nieuwenhuijs, E. Luijff, M. Klaver, Modeling Dependencies in Critical
793 Infrastructures, in: M. Papa, S. Sheno (Eds.), Critical Infrastructure
794 Protection II, Springer, 2008, pp. 205–213.
- 795 [43] E. E. Lee, J. E. Mitchell, W. A. Wallace, Restoration of services in interdepen-
796 dent infrastructure systems: A network flows approach, IEEE Transactions
797 on Systems, Man and Cybernetics Part C: Applications and Reviews 37
798 (2007) 1303–1317.
- 799 [44] J. P. Peerenboom, R. E. Fisher, Analyzing cross-sector interdependencies,
800 in: Proceedings of the Annual Hawaii International Conference on System
801 Sciences, 2007, pp. 1–9.
- 802 [45] G. E. Apostolakis, D. M. Lemon, A screening methodology for the identi-
803 fication and ranking of infrastructure vulnerabilities due to terrorism, Risk
804 Analysis 25 (2005) 361–376.
- 805 [46] L. Duenas-Osorio, J. Craig, B. Goodno, A. Bostrom, Interdependent response
806 of networked systems, Journal of Infrastructure Systems 13 (2007) 185–194.
- 807 [47] V. Latora, M. Marchiori, Efficient Behavior of Small-World Networks, Phys-
808 ical Review Letters 87 (2001) 3–6.
- 809 [48] M. Newman, Networks: An Introduction, 2 ed., Oxford University Press,
810 2018.
- 811 [49] G. Galvan, J. Agarwal, Vulnerability analysis of interdependent infrastruc-
812 ture systems, in: T. Haukaas (Ed.), Proceedings of the 12th International
813 Conference on Applications of Statistics and Probability in Civil Engineering
814 (ICASP12): Vancouver, Canada, July 12-15 University of British Columbia.,
815 2015.

- 816 [50] N. K. Svendsen, S. D. Wolthusen, Connectivity models of interdependency in
817 mixed-type critical infrastructure networks, Information Security Technical
818 Report 12 (2007) 44–55.
- 819 [51] N. K. Svendsen, S. D. Wolthusen, Analysis and statistical properties of
820 critical infrastructure interdependency multiflow models, Proceedings of the
821 2007 IEEE Workshop on Information Assurance, IAW (2007) 247–254.
- 822 [52] N. K. Svendsen, S. D. Wolthusen, Graph models of critical infrastructure
823 interdependencies, Lecture Notes in Computer Science 4543 LNCS (2007)
824 208–211.
- 825 [53] N. K. Svendsen, S. D. Wolthusen, An analysis of cyclical interdependencies
826 in critical infrastructures, Lecture Notes in Computer Science 5141 LNCS
827 (2008) 25–36.
- 828 [54] J. Williams, Identifying sensitive components in infrastructure networks via
829 critical flows, engrXiv (2019). URL: engrxiv.org/hyzbx. doi:[10.31224/
830 osf.io/hyzbx](https://doi.org/10.31224/osf.io/hyzbx).
- 831 [55] P. Novak, V. Guinot, A. Jeffrey, D. E. Reeve, Hydraulic Modelling – an
832 Introduction: Principles, Methods and Applications, Spon Press, 2010.
- 833 [56] P. Stride, Super sewer: an introduction to the Thames Tideway tunnel
834 project in London, Proceedings of the Institution of Civil Engineers - Civil
835 Engineering 169 (2016) 51–51.
- 836 [57] P. Stride, The Thames Tideway Tunnel: Preventing Another Great Stink, The
837 History Press, 2019.
- 838 [58] M. Amin, Toward Secure and Resilient Interdependent Infrastructures, Jour-
839 nal of Infrastructure Systems 8 (2007) 67–75.
- 840 [59] R. F. Austin, D. P. DiSera, T. J. Brooks, GIS for critical infrastructure pro-
841 tection, CRC Press, 2016.
- 842 [60] M. Mair, R. Sitzenfrei, M. Moderl, W. Rauch, Identifying multi-utility net-
843 work similarities, in: World Environmental and Water Resources Congress
844 2012: Crossing Boundaries, 2012, pp. 3147–3153.

- 845 [61] M. Mair, J. Zischg, W. Rauch, R. Sitzenfrei, Where to find water pipes
846 and sewers? - on the correlation of infrastructure networks in the urban
847 environment, *Water* 9 (2017).
- 848 [62] R. H. Shumway, D. S. Stoffer, *Time Series Analysis and Its Applications*,
849 Springer, 2017.
- 850 [63] R. Setola, S. Bologna, E. Casalicchio, V. Masucci, An Integrated Approach
851 for Simulating Interdependencies, in: M. Papa, S. Shenoi (Eds.), *Critical*
852 *Infrastructure Protection II*, Springer, 2008, pp. 229–242.
- 853 [64] T. Cormen, C. E. Leiserson, R. L. Rivest, C. Stein, *Introduction to Algo-*
854 *rithms*, 3 ed., MIT Press, Cambridge, MA, 2009.
- 855 [65] R. Ahuja, T. Magnanti, J. Orlin, *Network Flows: Theory, Algorithms, and*
856 *Applications*, Prentice Hall, Upper Saddle River, NJ, 1993.
- 857 [66] Aquacraft, *Embedded Energy in Water Studies, Study 3: End-use Water*
858 *Demand Profiles*, Technical Report, California Public Utilities Commission,
859 Energy Division, 2011.
- 860 [67] E. Zio, From complexity science to reliability efficiency: a new way of
861 looking at complex network systems and critical infrastructures, *International*
862 *Journal of Critical Infrastructures* 3 (2007) 488.